Infrared Physics & Technology 70 (2015) 34–39

Contents lists available at ScienceDirect

Infrared Physics & Technology

journal homepage: www.elsevier.com/locate/infrared

High image quality type-II superlattice detector for 3.3 μm detection of volatile organic compounds

Hedda Malm *, Anders Gamfeldt, Rickard Marcks von Würtemberg, Dan Lantz, Carl Asplund, Henk Martijn

IRnova AB, Electrum 236, SE-164 40 Kista, Sweden

ARTICLE INFO

Article history:
Received 6 August 2014
Available online 4 December 2014

Keywords:
Infrared detectors
Strained layer superlattice
Mid wave infrared
Barrier structure
InAs/GaSb
Volatile organic compounds (VOC)

ABSTRACT

Recent improvements in material quality, structure design and processing have made type-II superlattice a competing high end detector technology. This has also made it an attractive material of choice to meet the industrial need of high end gas detection, as for example detection of methane and other volatile organic compounds (VOC). A heterojunction structure with a cut off at 5 μm but intended for detection of VOC at 3.3 μm will be presented. The detector format is 320 × 256 pixels with 30 μm pitch using the ISC9705 read out circuit. The detector operability is 99.8% and NETD 12 mK (7 ms integration time, object temperature 30 °C and F#2.6, no cold filter used). The uniformity is at least on par with QWIP detectors. Anti-reflective coating is used and the substrate is fully removed. High quality imaging at operating temperature 110 K will be presented.

1. Introduction

Over the last ten years there has been a steady improvement of the detector technology type-II superlattice (T2SL), consisting of epitaxially grown layers of InAs and GaSb. This detector technology has the theoretical possibility of high quantum efficiency and low dark current, due in part to reduced interband tunneling and suppressed Auger generation, and in part to the many degrees of freedom in layer composition and thickness, which allows for efficient barrier designs by bandgap engineering. Progress in GaSb substrate quality [1,2], epitaxial structure design [3–6] and passivation [7–9] have made it possible to approach the performance of the competing detector technology Mercury Cadmium Telluride (MCT) [10]. This has also made it attractive for industrial applications.

An emerging industrial application for high end infrared detectors is gas detection. Many gases are transparent in the visible and most infrared wavelengths, but some gases have absorption in the infrared regions. These gases also radiate in the absorbed wavelengths region. By using a filter, the detection is limited to the region of interest and the contrast is increased. This method can be used for visualization and documentation in real time of gas leaks. In the long wave infrared range sulfur hexafluoride (SF_6) can be detected with a peak at 10.55 μm [11]. In the mid wave infrared range there is a large group of volatile organic compounds (VOC), for example methane, butane and propane with peaks around 3.3 μm that can be detected.

Methane makes up a considerable part of human greenhouse gas emission and about a third of the total methane emissions come from the production and distribution of natural gas and petroleum [12]. This makes the detection of methane leaks in this industry an important factor for reducing greenhouse emissions. Methane is also highly flammable and explosive if mixed with air, and undiscovered gas leaks have led to several lethal accidents.

Another very important reason for minimizing the release of VOCs into the air is the ability of VOCs to form ground level ozone when reacting with other pollutants such as nitrous oxide and carbon monoxide. Ground level ozone is a fundamental component in the formation of smog and is a huge problem for many of the world's largest cities. Although emission regulations can help, locating the sources of VOC emissions around and in cities can be very difficult limiting the enforceability of such regulations. Besides the environmental and safety aspects of gas leak detection, there is also an economic incentive to reduce the gas lost in leaks in for example natural gas distribution.

The use of infrared imaging for gas leak detection has several advantages over traditional "sniffing" type instruments (where the instrument needs to be in direct contact with the gas to be detected). The technical principle behind this technique is to make use of the absorption that many gases have in certain infrared spectral bands. By fine tuning the detection band of an infrared

* Corresponding author. Tel.: +46 8 793 66 14; fax: +46 8 519 02518.
E-mail address: hedda.malm@ir-nova.se (H. Malm).

http://dx.doi.org/10.1016/j.infrared.2014.11.013
1350-4495/

imager the otherwise invisible gas appears clearly in the infrared image.

Such a device gives the operator an actual live video of the equipment to be surveyed, with any leaks appearing as dark or light clouds in the image. Obviously, this means large areas or big equipment can much more easily be scanned for leaks than if using a sniffing device. When scanning for explosive or toxic gases, the possibility to do the survey from a safe distance is also an important advantage.

To match existing read out circuits (ROIC), mainly p-on-n detector structures are used to make T2SL FPAs. That is also the case for the VOC detector described in this paper. However, a comparison was made to an n-on-p structure in order to evaluate the detector material properties.

2. Experiment

Two heterojunction p-i-n-diodes were epitaxially grown on 3-inch n-type (Te-doped) GaSb (100) substrates using solid source molecular beam epitaxy (MBE).

Structure A consists of a 0.3 μm lattice matched $InAs_{0.91}Sb_{0.09}$ etch-stop layer followed by 0.7 μm heavily Si-doped n-type "M-superlattice" (M-SL) bottom contact, 0.5 μm lightly doped n-type M-SL, 3.9 μm weakly doped p-type SL absorber, 0.1 μm of heavily Be-doped p-type SL, and finally a 0.1 μm thick heavily Be-doped p-type GaSb contact layer. The M-SL periods consist of InAs/GaSb/AlSb/GaSb in the proportions 10/1/4/1 monolayers (ML), whereas the absorber SL consists of 10 ML InAs/ 11.5 ML GaSb. The top and bottom contacts are doped to 2×10^{18} cm^{-3} and 6×10^{17} cm^{-3} respectively, and the doping concentration in the absorber is 3×10^{16} cm^{-3} (p-type). This is a slightly modified and improved version of the epitaxial design reported in [13], as explained in detail in [15]. A calculated band edge diagram for this structure is shown in Fig. 1.

Structure B was also grown on n-type (Te-doped) GaSb (100) substrates using MBE with the aim of producing an inverted version of Structure A describe above. Structure B consists of a 0.3 μm lattice matched $InAs_{0.91}Sb_{0.09}$ etch-stop layer, heavily Si-doped to 2×10^{18} cm^{-3} followed by a 1 μm thick p-type bulk GaSb contact and a 0.1 μm p-SL contact, a 3.9 μm weakly doped p-type SL absorber, 0.5 μm lightly doped n-type M-SL barrier and finally a n-SL top contact. The M-SL period design and the absorber SL design are both equal to the ones in Structure A, including doping concentrations. The top and bottom contacts are doped to 6×10^{17} cm^{-3} and 2×10^{18} cm^{-3} respectively.

Single pixel detectors of sizes from 30×30 μm^2 to 190×190 μm^2 were produced using standard III/V processing techniques. The pixels were formed by a combination of dry and wet etching [14] and passivated using a dielectric passivation [15]. Mirror and contact metal was evaporated onto the pixels and the chip was glued to a PCB.

Using the same processing methods, 320 × 256 pixels detector arrays with 30 μm pixel pitch were produced out of Structure A. Stepper lithography was used to define the pixels in this case. Mirror, contact metal and indium bumps were evaporated onto the pixels before dicing. The arrays were then hybridized to the read out circuit ISC9705, underfill was deposited and finally the GaSb substrate was fully removed. The focal plane arrays (FPA) are using an antireflective coating optimized for detection at 3.3 μm.

The FPAs were then mounted on a ceramic carrier, wire-bonded and put in a cooled test dewar with F#2.6 for tests of imaging performance. When applicable, a cold passband filter at 3.1–3.575 μm was used.

3. Results and discussion

The external quantum efficiency of Structure A at 100 K with antireflection coating optimized for 3.3 μm wavelength is shown in Fig. 2. The complete absence of bias dependence shows that minority electrons flow unobstructed from absorber into the M-SL barrier – i.e. there is no barrier in the SL conduction band.

The effect of the antireflection coating is illustrated in Fig. 3 where the external quantum efficiency of Structure A was measured on focal plane arrays with light entering from the backside. The cut-off wavelength is dependent on temperature but there is very little temperature dependence below 4.5 μm. The standing wave pattern is due to optical interference between the air/semiconductor interface and the semiconductor/metal interface on the bump side.

The solid line of Fig. 4 shows the calculated background limited spectral detectivity (D^*) of Structure A (with an AR-coating optimized for 3–5 μm) at 100 K based on the measured quantum efficiency. The dashed line indicates the peak spectral D^* for an ideal photo voltaic detector as a reference. Note that the peak value of 1.1×10^{11} cm $tHz^{1/2}/W$ occurs at a shorter wavelength than the cut-off wavelength $\lambda_{co,90\%} = 5.3$ μm of the device. This is due to the lower quantum efficiency towards the cut-off. At 100 K, the background photon noise is the predominant noise source and Johnson noise or other noise sources do not play a significant role.

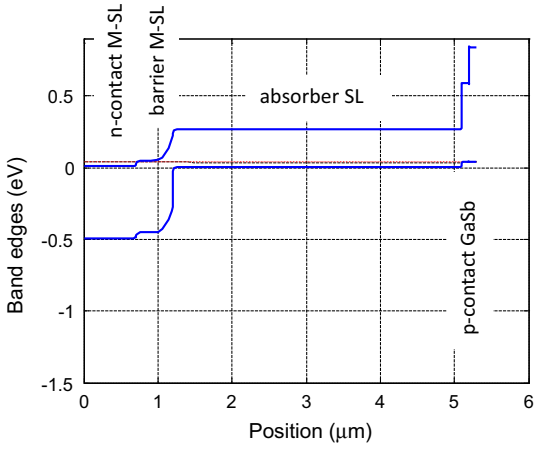

Fig. 1. Calculated band edges for Structure A under zero bias. Light enters from the left. The etch stop layer is not shown.

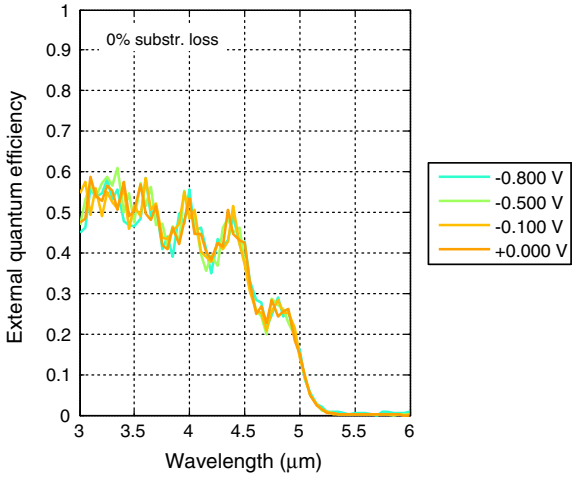

Fig. 2. External quantum efficiency of Structure A at 100 K with antireflection coating optimized for 3.3 μm wavelength.